

ELECTROCHEMICAL STUDIES OF 1-FERROCENYLMETHYL-3-METHYL- IMIDAZOLIUM IODIDE AND 1-(FERROCENYLMETHYL)-3-MESITYL- IMIDAZOLIUM IODIDE: REDOX POTENTIAL AND SUBSTITUENT EFFECTS

Neghmouche Nacer Salah^{1,2*}, Rebiai Abdelkrim¹, De Frémont Pierre³, Dagonne Samuel³ and Louafi Fadila^{2*}

¹University of El Oued, Department of Chemistry, P.O. Box 789, 39000, El Oued, Algeria

²Unité de Recherche CHEMS, Université des frères Mentouri de Constantine 1, Constantine, 25000, Algeria

³Equipe de Synthèse, Réactivité et Catalyse Organométalliques (UMR 7177 CNRS), Université de Strasbourg, 4 rue Blaise Pascal, CS 90032, 67081 Strasbourg, France

(Received December 2, 2019; Revised December 5, 2020; Accepted January 4, 2021)

ABSTRACT. The electrochemical behavior of 1-ferrocenylmethyl-3-(methyl)-imidazolium iodide (or mesityl) imidazolium was studied by cyclic voltammetry at glassy carbon electrode in midiums organic to determine the influences of electronic imidazolium group on the ferrocene. The experimental results indicated that the redox reaction was reversible. Mass transport towards the electrode is a simple diffusion process and the diffusion coefficient (D) for redox couple has been also calculated and we have evaluated the heterogeneous charge transfer rate constant (K^0).

KEY WORDS: Electrochemical behaviour, Cyclic voltammetry, Imidazolium salts, Diffusion coefficient

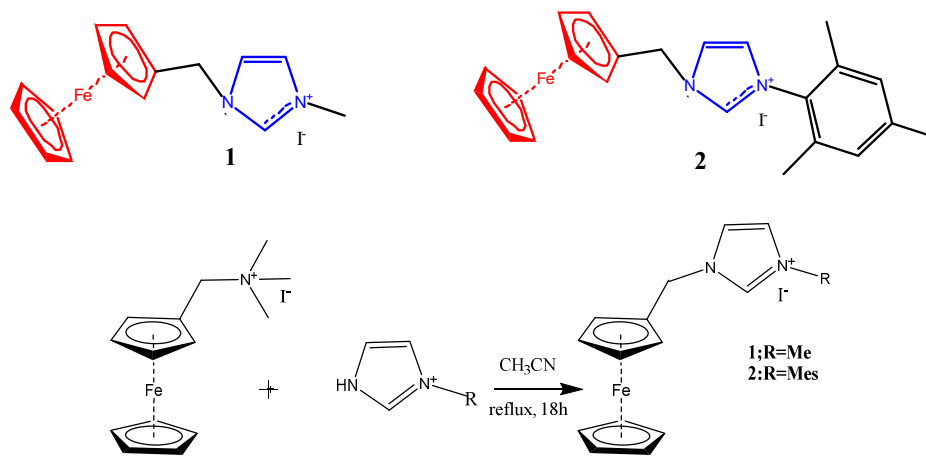
INTRODUCTION

During the past several years, ionic liquids have developed particularly well because of their many interesting physicochemical properties [1], such as low saturation vapor pressure, limited viscosity, low miscibility with most common solvents, supramolecular arrangement, which make them powerful tools in many fields of chemistry. Imidazolium salts are the largest family of ionic liquids to date [2]. Their modulability allows them to be derived for many specific applications, especially in organic synthesis, where they are mainly used as solvents, and more recently as catalysts [3]. The first example of an air- and water-stable imidazolium salt was reported in 1992 by Wilkes and Zaworotko [4]. All these properties of ionic liquids made interesting in rechargeable batteries [5], it showed a potential alternative to lithium-ion batteries and lithium sulfate played a role in improving the ability to use conventional electric batteries [6-7]. The electrochemical stability of electrolytes, defined as the difference between solvent and oxidation reduction potentials, plays an important role on a large scale [8]. The selection of cathodic and anode materials for use in high-energy high-density batteries is limited by electrochemical stability [9], resulting in oxidation or reduction of the electrolyte within the potential of the anode and cathode electrodes. This problem can be solved by the use of more electrochemical stable electrolytes. Experimental studies have shown that many ionic liquids appear high conductivity. Moreover, given the large number of potential absorption processes of cations and anions that form ionic liquids with a wide range of electrochemical properties, the application of an effective method such as the known thermal cycle approach will significantly reduce the time and cost associated [8, 10]. In a previous study ferrocene was used as an electronic storage unit in oxidation flow batteries by standard reduction potentials for different species comparisons [11, 12]. Ferrocene, has a redox potential of Fc^+/Fc^0 of $E_{1/2} = +514$ mV at ESC electrode [13]. In our study, we have prepared two ferrocenyl imidazolium salts **1**, **2**

*Corresponding author. E-mail: neghmouchenacer-salah@univ-eloued.dz

This work is licensed under the Creative Commons Attribution 4.0 International License

(Scheme 1) and tested them by cyclic voltammetry technique to calculate their electrochemical constants.



Scheme 1. Synthesis of **1** and **2**.

EXPERIMENTAL

Syntheses of 1-ferrocenylmethyl-3-methyl-imidazolium iodide

The imidazolium salt was synthesized by modifying a published procedure [14]. A solution of 1-ferrocenylmethyl)trimethylammonium iodide (5 g, 13.00 mmol) and the appropriate methylimidazole (14.3 mmol) in anhydrous MeCN (10 mL) was refluxed for 18 h. The cooled solution was poured into water (50 mL) and extracted with chloroform (3 x 25 mL). The extracts were washed with water (2 x 50 mL), dried (MgSO_4) and evaporated to give an orange oil. Diethyl ether (50 mL) was then added and the desired salts precipitated on scratching. The yellow solid was collected by filtration, washed with diethyl ether and dried at room temperature. (Scheme 1) (6.5 g, yield $\frac{1}{4}$ 72%). $^1\text{H-NMR}$ ($\text{CDCl}_3\text{-d}_6$, δ , ppm): 4.04 (s, 3H, CH_3), 4.25 (s, 7H, Cp H), 4.47 (s, 2H, Cp H), 5.36 (s, 2H, Fc- CH_2 -), 7.27 (s, 1H, 5-Im H), 7.32 (s, 1H, 4-Im H), 9.93 (s, 1H, 2-im H). $^{13}\text{C NMR}$ ($\text{CDCl}_3\text{-d}_6$, δ , ppm): 37.16 (NCH_3), 50.2 (Fc- CH_2 -), 69.35-78.4 (Cp C-H and Cp C-C), 121.51 (4-h C), 123.2 (5-h C), 136.26 (2- Im C). Anal. calcd for $\text{C}_{15}\text{H}_{17}\text{N}_2\text{IFe}$: C, 44.15; H, 4.2%; found: C, 44.20; H, 4.18%.

Syntheses of 1-(ferrocenylmethyl)-3-mesityl-imidazolium iodide [15]

A 100 mL Schlenk flask equipped with a reflux condenser was charged with a stir bar, 1-ferrocenylmethyl)trimethylammonium iodide (1.5 g, 3.9 mmol), 1-(mesityl)imidazole (0.798 g, 4.3 mmol), and anhydrous CH_3CN (10 mL). The resulting solution was heated at reflux for 24 h, during which time a dark brown color formed. Afterward, the volatiles were removed under reduced pressure and the resulting brown solid was extracted with CH_2Cl_2 (15 mL) and then washed with deionized water (5×10 mL) to remove unreacted starting material. The organic layer was collected, evaporated under reduced pressure, and the residual brown solid was washed with Et_2O (3×5 mL). Recrystallization with $\text{CH}_2\text{Cl}_2/\text{Et}_2\text{O}$ (1:5 v:v) at -20 °C yielded the desired product as yellow crystals (1.65 g, 83%). $^1\text{H-NMR}$ (DMSO-d_6 , δ , ppm): 1.98 (s, 6H,

ortho 2CH₃); 2.32 (s, 3H, para-CH₃); 4.25-4.28 (s, 7H, Cp H); 4.46 (s, 2H, C_p); 5.27 (s, 2H, Fc-CH₂-); 7.14 (s, 2H, meta Ar-H); 7.91 (s, 1H, 5-Im H); 8.05 (s, 1H, 4-Im H); 9.47 (s, 1H, 2-im H). ¹³C-NMR (DMSO-d₆, δ, ppm): 16.92 (ortho 2CH₃); 20.61 (para-CH₃); 48.9 (Fc-CH₂); 68.63 (C_p); 68.78 (C_p); 68.97 (C_p); 81.1 (C_p-C). 123.02 (meta 2C_{Ar}); 123.97 (ortho 2C_{Ar}); 129.28 (para-C_{Ar}); 131.2 (C_{Ar}-N); 134.24 (C=C); 136.95 (C=C); 140.31 (C=N imi). Anal. calcd for C₂₃H₂₅N₂IFe: C, 53.93; H, 4.92; N, 5.47%; found: C, 53.81; H, 4.93; N, 5.42.

Electrochemical measurement

The cyclic voltammetry measurements were performed in a heart-shaped electrochemical cell using a PGZ-402 potentiostat. The electrodes were glassy carbon, platinum wire and Hg/Hg₂Cl₂ wire as the working, counter and reference electrodes, respectively. The solutions were degassed with argon for about 3 min before each experiment. All measurements are referenced against the E_{1/2} of the Fc/Fc⁺ redox couple. Nicholson and Gileadi methods were used for heterogeneous electron transfer rate constant. Randles-Sevcik equation was used to determine diffusion coefficient and number of electrons involved in the electrode process [16].

We chose CH₃CN as a solvent. The purpose of the support electrolytes is to ensure the electrical conductivity in the solution to be studied. The carrier electrolyte used in our study is tetrabutylammonium tetrafluoroborate (Bu₄NBF₄) in CH₃CN and studied the electroactivity the system contains background salt in acetonitrile. The voltammograms obtained are shown in Figure 1.

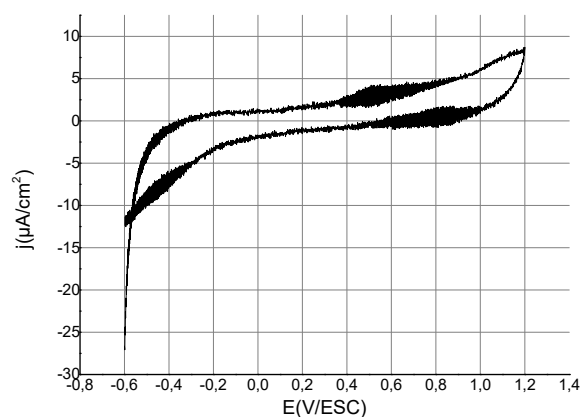


Figure 1. Cyclic voltammogram CH₃CN//Bu₄NBF₄ 0,1 M, on glassy carbon electrode, recorded between 0 and +1400 mV / ECS at $\nu = 100$ mV/s.

RESULTS AND DISCUSSION

Electrochemical behavior study of 1 and 2

The cyclic voltammogram of the 1-ferrocenylmethyl-3-methylimidazolium iodide derivative (1) is recorded in a potential range from 0 to 1.1 V at a scanning rate of 100 mV.s⁻¹ (Figure 2). On this voltammogram, two anodic peaks are noted: the first is at 0.296 V, relative to the oxidation of the imidazolium function, the second is at 0.615 V, relative to the oxidation of the ferrocenium/ferrocene redox couple Fc⁺/Fc. A cathode peak is observed at 0.517 V, attributed to the reduction of ferrocenium/ferrocene Fc⁺/Fc redox couple. As for the derivative 1-ferrocenylmethyl-3-mesityl-imidazolium iodide (2) the same thing, the anodic peaks in 0.340 V and 0.613 V, a cathodic peak is observed at 0.528 V.

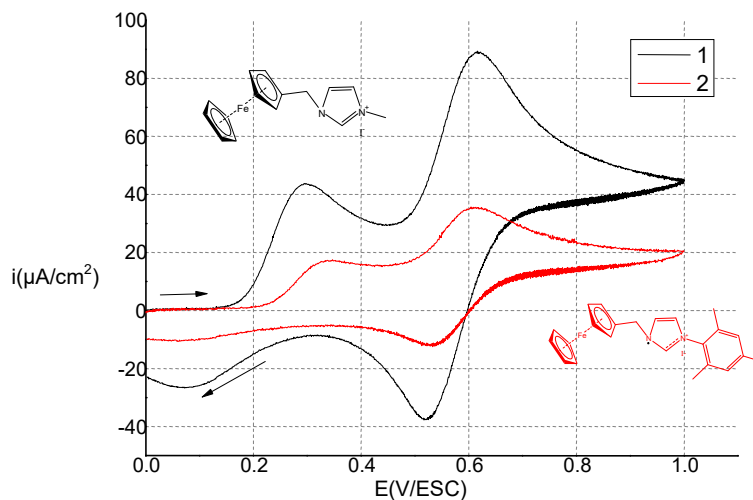


Figure 2. Cyclic voltammograms (0.1 M $\text{CH}_3\text{CN}/\text{Bu}_4\text{NBF}_4$, scan rate = 100 mV s^{-1}) of compounds **1** and **2**.

Effect of scan rate

Figure 3 shows the voltammograms recorded on a glassy carbon electrode at different scan rates around the Fc/Fc^+ pair. This pair exhibits a reversible behavior in 0.1 M ($\text{CH}_3\text{CN}/\text{Bu}_4\text{NBF}_4$). Indeed, the ratio of the intensity of the reduction and oxidation peaks is approximately equal to 1 and the intensities evolved linearly with the square root of the scan rates as shown in the insert in Figure 4. However, it is noted that the difference between the potentials of the reduction and oxidation peaks increases with the scanning speed. The ΔE_p values of 96 mV (compound **1**), 75 mV (compound **2**) are recorded for a scan rate of 40 mV/s and 98 mV (compound **1**), 85 mV (compound **2**) for a scan rate of 100 mV/s. Even for low scanning speeds, there is therefore a difference much greater than the theoretical deviation of $2.3RT/nF$ (i.e. 59 mV at 25 °C) for a perfectly reversible system. It should be noted that this difference is, in part, due to the non-compensation of the ohmic drop.

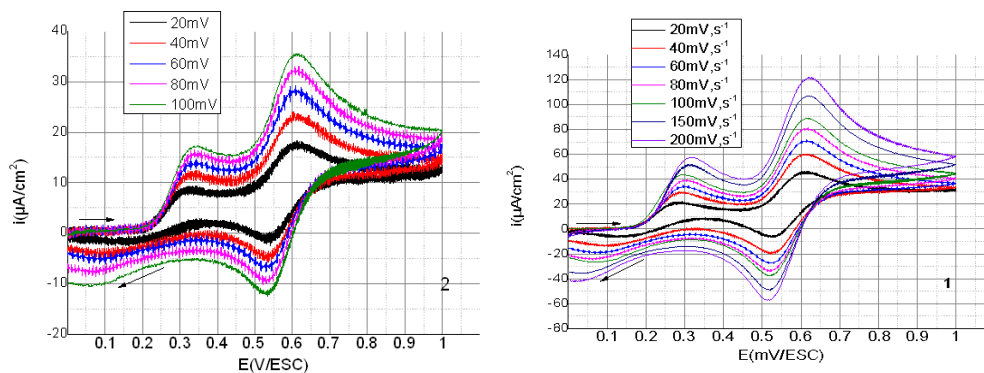


Figure 3. Cyclic voltammograms in (0.1 M $\text{CH}_3\text{CN}/\text{Bu}_4\text{NBF}_4$) of compounds **1** and **2** at different scan rates.

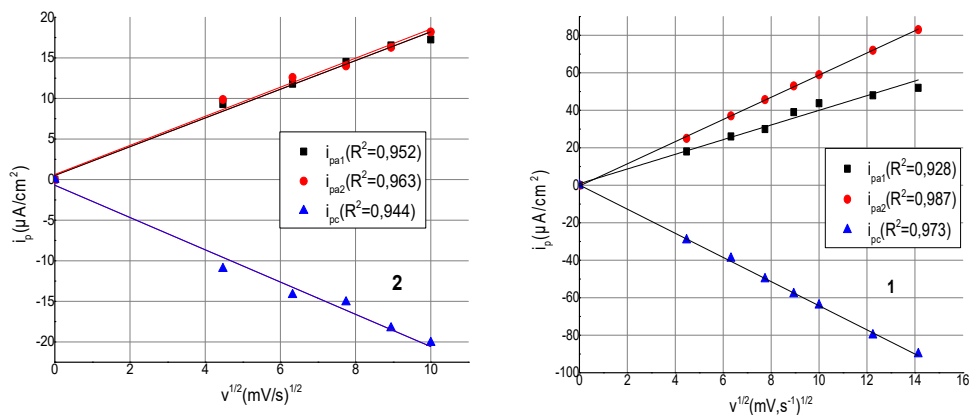


Figure 4. Plot of current maximum against square root of scan rate for compounds **1** and **2**.

Cyclic voltammograms are obtained at a series of voltage scan rates and a plot of peak current versus $v^{1/2}$ is prepared. The plot should be linear with zero intercept. The slope is equal to $2.69 \times 10^5 \text{ ACD}^{1/2}$. Thus, the value of D can be obtained if the electrode area is known (1 cm^2) (Table 1). These diffusion coefficients have been corrected according to the experimentally determined percentage of ligand exchange.

The electrochemical stability of the derivatives **1** and **2** are confirmed by a successive scanning of the potential between 0 and 1.1 V ($v = 20, 40, 60, 80, 100, 150, 200 \text{ mv.s}^{-1}$) and shows the decrease of the intensity of the peak current as the scanning speed decreases. The electrochemical parameters calculated from voltammograms are summarized in Table 2.

Table 1. Diffusion coefficients of **1** and **2** clusters calculated from cyclic voltammograms obtained using a GC working-electrode in $\text{CH}_3\text{CN}/\text{Bu}_4\text{NBF}_4$ (0.1 M) supporting electrolyte.

Compound	$D_o \cdot 10^{-7} \text{ (cm}^2 \cdot \text{s}^{-1}\text{)}$	$D_R \cdot 10^{-7} \text{ (cm}^2 \cdot \text{s}^{-1}\text{)}$
1	4.69	5.69
2	4.60	6.39

Table 2. Voltammetric data for **1** and **2** in 0.1 M ($\text{CH}_3\text{CN}/\text{Bu}_4\text{NBF}_4$).

Compounds	v mV/s	i_{pa1} $\mu\text{A}/\text{cm}^2$	i_{pa2} $\mu\text{A}/\text{cm}^2$	i_{pc} $\mu\text{A}/\text{cm}^2$	E_{pa1} mV	E_{pa2} mV	E_{pc} mV	ΔE_p mV	$E_{\frac{1}{2}}$ mV	$\left \frac{i_a}{i_c} \right $
1	20	18	25	-29.25	293	615	518	95	566.5	0.86
	40	26	37	-39.2	296	614	518	96	566	0.95
	60	30	45.7	-50.1	296	615	516	99	565.5	0.91
	80	39	52.6	-58	295	614	519	95	566.5	0.91
	100	43.75	59	-64.2	296	615	517	98	566	0.92
	150	48	72	-79.1	297	616	516	100	566	0.91
	200	52	83	-90.3	302	616	518	98	567	0.92
2	20	9.3	8.2	-10.99	315.5	608.75	544.25	70.25	579.37	0.9
	40	11.81	11.6	-14.2	328.5	610.5	537	75	574	0.89
	60	14.51	14	-15.1	344.3	611.8	530.6	75.6	568.4	0.93
	80	16.54	16.3	-18.3	338.6	612.5	530.2	82.3	571.35	0.89
	100	17.263	18.2	-20.1	340	613	528	85	570.5	0.91

To find out about the reaction mechanism at the electrode, variations in the intensity of the anodic and cathodic current were studied as a function of the square root of the scanning speed. The straight line pattern of (I_{pa}) and (I_{pc}) versus the square root of the scanning rate for the two imidazolium derivatives **1** and **2** confirms that the electrochemical reaction on the electrode is controlled by diffusion.

Diffusion coefficient (D)

The diffusion coefficient (D) was calculated from CV measurements of the cathodic peak current of a reversible or quasi-reversible system using the Randles-Sevcik Eq.

$$i_p = 0.4463nFAC \left(\frac{nF}{RT} \right)^{1/2} D^{1/2} v^{1/2} \quad (1)$$

where n is the number of electrons, in this case one, F is the Faraday constant (96485.332 C mol⁻¹), A is the electrode area (cm²), C is the concentration (mol/cm³), R is the gas constant (J K⁻¹ mol⁻¹), T is the temperature, v is the scan rate and D is the diffusion coefficient.

In equation 1, i_p is the peak current in amperes, and v is the potential scan rate in V/s. For a one-electron transfer at 25 °C, this becomes Eq. (2):

$$i_p = 2.69 \times 10^5 ACD^{1/2}v^{1/2} \quad (2)$$

Heterogeneous electron transfer rate constant (k^0)

All electrochemical processes proceed via a transition state (ts) which is less stable than both reactants and products. α is an indication of how reactant-like or product-like the (ts) is in terms of its electrical behaviour. The value of α lies between zero and one. It is often (but not always) around 0.5. If it is close to either of the two extremes (zero or one), we can say that the ts is either very reactant-like or very product-like. The rate constant for an electrochemical process depends exponentially on both the electrode potential and α .

Heterogeneous rate constants for the pure ferrocene and its derivatives were calculated by using relationship between the rate constant for heterogeneous electron transfer and peak separation formulated as given below [19].

Nicholson [20, 21] method is used frequently to determine standard heterogeneous electron transfer rate constant k^0 by relating it with a dimensionless kinetic parameter Ψ (Eq. (3)).

$$k^0 = \psi \left[\frac{\pi D_o \frac{nFv}{RT}}{\gamma^\alpha} \right]^{1/2} \quad (3)$$

where $\gamma = (D_o / D_R)^{1/2}$ and $\alpha = 0.5$. The value of α is nearly independent for reversible reactions. Kochi [22] has reported the following expression (Eq. (4)).

$$k^0 = 2.18 \left[\frac{\alpha D_o nFv}{RT} \right]^{1/2} \exp \left[\frac{-\alpha^2 nF(E_{pa} - E_{pc})}{RT} \right] \quad (4)$$

A comparatively simpler method for the evaluation of k^0 is Gileadi's [23, 24] method; then following Eq. (5) is used to calculate the value of k^0 (Table 3):

$$\log(k^0) = -0.48\alpha + 0.52 + \log \left[\frac{\alpha D_o nFv}{2.303RT} \right]^{1/2} \quad (5)$$

Table 3. Values of k^0 determined from Nicholson and Gileadi's method.

Compounds	v (V/s)	ΔE_p (mV)	ψ	k^0 ($\text{cm}\cdot\text{s}^{-1}$)	Average (k^0) $\text{cm}\cdot\text{s}^{-1}$
1	0.02	95	1	3.56	4.78
	0.04	96	0.82	4.14	SD = 0.278
	0.06	99	0.73	4.52	
	0.08	95	0.68	4.81	
	0.1	98	0.63	5.05	
	0.15	100	0.57	5.52	
	0.2	98	0.52	5.87	
2	0.02	70.25	0.97	3.53	4.37
	0.04	75	0.8	4.1	SD = 0.232
	0.06	75.6	0.71	4.48	
	0.08	82.3	0.66	4.77	
	0.1	85	0.61	5.00	

CONCLUSION

Two 1-ferrocenylmethyl-3-alkyl imidazolium iodide salts were synthesized, where the alkyl group included the following: methyl and mesityl groups. This synthesis was verified by standard chemical techniques, proton NMR spectroscopy, and carbon NMR spectroscopy. The electrochemical behavior of these salts was performed in acetonitrile at 298.15 K using cyclic voltammetry to evaluate the kinetic parameters. The estimated values of heterogeneous rate constants (k^0) and diffusion coefficients (D) showed the presence of strong interactions between the ferrocene and the imidazolium group. They indeed exhibit reversible redox characteristics, which indicate that ferrocene based salts, which melt at low temperatures, are a class of compounds that are worthy of additional study for their battery applications.

ACKNOWLEDGEMENT

This work was supported by the ministry of higher education and scientific research of Algeria (code B00L01UN250120180011).

REFERENCES

1. Zhou, Q.; Lu, X.; Zhang, S.; Guo, L. Physicochemical properties of ionic liquids. *Korean J. Chem. Eng.* **2017**, 34, 425-439.
2. Kowsari, M.H.; Alavi, S.; Ashrafizaadeh, M.; Najafi, B. Molecular dynamics simulation of imidazolium-based ionic liquids. II. Transport coefficients. *J. Chem. Phys.* **2009**, 130, 014703.
3. Trillo, P.; Pastor, I.M. Iron-based imidazolium salts as versatile catalysts for the synthesis of quinolines and 2- and 4-allylanilines by allylic substitution of alcohols. *Adv. Synth. Catal.* **2016**, 358, 2929-2939.
4. Wilkes, J.S.; Zaworotko, M.J. Air and water stable 1-ethyl-3-methylimidazolium based ionic liquids. *J. Chem. Soc. Chem. Commun.* **1992**, 965-967.
5. Zhu, G.; Angell, M.; Pan, C.-J.; Lin, M.-C.; Chen, H.; Huang, C.-J.; Lin, J.; Achazi, A.J.; Kaghazchi, P.; Hwang, B.-J.; Dai, H. Rechargeable aluminum batteries: effects of cations in ionic liquid electrolytes. *RSC Adv.* **2019**, 9, 11322-11330.

6. Peng, C.; Liu, F.; Wang, Z.; Wilson, B.P.; Lundström, M. Selective extraction of lithium (Li) and preparation of battery grade lithium carbonate (Li_2CO_3) from spent Li-ion batteries in nitrate system. *J. Power Sources* **2019**, 415, 179-188.
7. Sieber, T.; Ducke, J.; Rietig, A.; Langner, T.; Acker, J. Recovery of $\text{Li}(\text{Ni}_{0.33}\text{Mn}_{0.33}\text{Co}_{0.33})\text{O}_2$ from lithium-ion battery cathodes: Aspects of degradation. *Nanomaterials* **2019**, 9, 246.
8. Kazemiabnavi, S.; Zhang, Z.; Thornton, K.; Banerjee, S. Electrochemical stability window of imidazolium-based ionic liquids as electrolytes for lithium batteries. *J. Phys. Chem. B* **2016**, 120, 5691-5702.
9. Borodin, O.; Ren, X.; Vatamanu, J.; Von Wald Cresce, A.; Knap, J.; Xu, K. Modeling insight into battery electrolyte electrochemical stability and interfacial structure. *Acc. Chem. Res.* **2017**, 50, 2886-2894.
10. Li, Q.; Chen, J.; Fan, L.; Kong, X.; Lu, Y. Progress in electrolytes for rechargeable Li-based batteries and beyond. *Green Energy Environ.* **2016**, 1, 18-42.
11. Matsubara, Y. Standard electrode potentials for the reduction of CO_2 to CO in acetonitrile-water mixtures determined using a generalized method for proton-coupled electron-transfer reactions. *ACS Energy Lett.* **2017**, 2, 1886-1891.
12. Isse, A.A.; Lin, C.Y.; Coote, M.L.; Gennaro, A. Estimation of standard reduction potentials of halogen atoms and alkyl halides. *J. Phys. Chem. B* **2011**, 115, 678-684.
13. Gagne, R.R.; Koval, C.A.; Lisensky, G.C. Ferrocene as an internal standard for electrochemical measurements. *Inorg. Chem.* **1980**, 19, 2854-2855.
14. Howarth, J.; Thomas, J.-L.; Hanlon, K.; McGuirk, D. 1,3-Di(ferrocenylmethyl)imidazolium and 1-ferrocenylmethyl-3-alkylimidazolium salts: A high yield and facile synthesis. *Synth. Commun.* **2000**, 30, 1865-1878.
15. Arumugam, K.; Varnado, C.D.; Sproules, S.; Lynch, V.M.; Bielawski, C.W. Redox-switchable ring-closing metathesis: Catalyst design, synthesis, and study. *Chem. Eur. J.* **2013**, 19, 10866-10875.
16. Naima, B.; Abdelkrim, R.; Ouarda, B.; Salah, N.N.; Larbi, B.A.M. Chemical composition, antimicrobial, antioxidant and anticancer activities of essential oil from *Ammodaucus leucotrichus* Cosson & Durieu (Apiaceae) growing in South Algeria. *Bull. Chem. Soc. Ethiop.* **2019**, 33, 541-549.
17. Alemu, H.; Abegaz, B M.; Bezabih, M. Electrochemical behaviour and voltammetric determination of *geshoidin* and its spectrophotometric and antioxidant properties in aqueous buffer solutions. *Bull. Chem. Soc. Ethiop.* **2007**, 21, 189-204.
18. Sawyer, D.T.; Sobkowiak, A. Roberts, J.L.. *Electrochemistry for Chemists*. 2nd ed., John Wiley and Sons Inc.: New York; **1995**.
19. Ortiz, M.E.; Nunez-Vergara, L.J.; Squella, J.A. Voltammetric determination of the heterogeneous charge transfer rate constant for superoxide formation at a glassy carbon electrode in aprotic medium. *J. Electroanal. Chem.* **2003**, 549, 157-160.
20. Bard, A.J.; Faulkner, L.R. *Electrochemical Methods, Fundamentals and Applications*, John Wiley and Sons: New York; **1980**, pp. 218.
21. Moharram, Y.I. Extraction of electrode kinetics and transport parameters of ferrocene at a platinum electrode from semiintegral electroanalysis. *J. Electroanal. Chem.* **2006**, 587, 115-126.
22. Golabi, S.M.; Zare, H.R.; Hamzehloo, M. Electrocatalytic oxidation of hydrazine at a pyrocatechol violet (PCV) chemically modified electrode. *Microchem. J.* **2001**, 69, 13-23.
23. Haji, M.; Iftikhar, A.T.; Mehboob, M.; Zaheer, M.; Muhammad, A.V.; Obaid, K.; Muhammad, L.; Muddasir, H. A comprehensive heterogeneous electron transfer rate constant evaluation of dissolved oxygen in DMSO at glassy carbon electrode measured by different electrochemical methods. *J. Electroanal. Chem.* **2016**, 775, 157-162.
24. Bockris, J.O.M.; Reddy, A.K.N. *Modern Electrochemistry*. Vol. 1, Plenum Press: New York; **1977**.